Heritage Science

RESEARCH

Open Access

Experimental study on the effects of hydrochemistry and periodic changes in temperature and humidity on sandstone weathering in the Longshan Grottoes

Bo Sun[1,2,3], Xingyue Li[1,2], Kai Cui[2], Jie Hong[1,3], Rui Chen[1], Chen Jia[5] and Ningbo Peng[3,4*]

Abstract

Changes in precipitation, temperature and humidity can lead to the weathering of rock masses in grottoes; these changes are common in sandstone grottoes. To simulate this cyclic process, different salt solutions were designed according to the main precipitated components. Sandstone specimens taken from Longshan Grottoes were soaked in these solutions for 48 h and then placed in a simulated environment with temperature and humidity changes for 5 cycles (50 h) to study the effects of hydrochemical, temperature and humidity changes on the sandstone. Physical indexes, such as mass, wave velocity, surface hardness and tensile strength, of the rock samples were measured every three cycles, and the damage characteristics and mechanisms of the sandstone were discussed based on SEM and XRD test results. The results showed that the macroindicators and microstructures of the samples gradually decreased with increasing number of cycles. The physical indexes of the rock samples in different solutions changed at different rates, the changes in surface hardness and tensile strength were consistent, and the responses were less sensitive to deterioration than to longitudinal wave velocity. In different solutions, the microstructures and mineral compositions of the samples showed different trends with increasing number of cycles. This damage was caused by a combination of various actions, such as feldspar dissolution, chemical erosion, water scouring, clay mineral expansion and disintegration, and salt crystallization, which increased the number of pores, enlarged the holes and expanded the cracks inside the rock samples.

Keywords Longshan Grottoes, Sandstone, Change in temperature and humidity, Water-chemical environment, Weathering

*Correspondence:
Ningbo Peng
pengnb@hyit.edu.cn
[1] Northwest Research Institute Limited Company of China Railway Engineering Corporation, Lanzhou 730000, Gansu, China
[2] Key Laboratory of Disaster Prevention and Mitigation in Civil Engineering, Lanzhou University of Technology, Lanzhou 730050, Gansu, China
[3] Faculty of Architecture and Civil Engineering, Huaiyin Institute of Technology, Huaian 223001, Jiangsu, China
[4] Institute for Conservation of Cultural Heritage, Shanghai University, Shanghai 200444, China
[5] Taiyuan Cultural Relics Protection and Research Institute, Taiyuan 030012, Shanxi, China

Introduction

The Longshan Grottoes situated at the summit of Longshan Mountain in Jinyuan District, Taiyuan City. This collection stands as the largest existing pure Taoist grotto group. In 1996, the Longshan Grottoes were rightfully recognized and included in the fourth group of the National Key Cultural Relics Protection Units in China. The Longshan Grottoes have been exposed to open air for a long time, and they have been affected by various natural factors. The grotto sandstone has undergone numerous weathering processes, including large-scale powdering, plate-like peeling, and layered

peeling. This kind of weathering is common in grotto sandstone worldwide. According to the investigations and indoor experimental studies of the present environment of the Longshan Grottoes, the damage mechanism of the sandstone in the freeze–thaw environment has been preliminarily clarified [1]. However, surface sandstone weathering is not only related to the freeze–thaw and chemical erosion caused by the decrease in winter temperature and snowfall, but also closely related to the weathering effect caused by changes in the water, including those in the chemical environment, daily humidity, and rainfall.

To date, much research has been performed on water–rock interactions [2–10]. Usually, the methods used by researchers include immersion drying, with immersion times usually being set at 24 h [2–4], 48 h [5, 6], 12 h [7], and 96 h [8]; the drying temperature is set in ranges of either 100–110 °C [3, 6–8] or 50–60 °C [2, 4, 5], and the drying time is either 24 h [2–4, 6, 8] or 12 h [5, 7]. On this basis, some scholars have adjusted the experimental conditions by soaking and drying at room temperature for repeated wetting and drying cycles [9]. In addition, some scholars have conducted experiments according to the local daily average humidity changes by performing wind drying during the day (9:00 ~ 21:00) and immersion at night (21:00–9:00)[10] (Table 1).

Most scholars adopt long-term immersion in different chemical solutions [11, 12] or in solutions with different pH values instead of distilled water for dry–wet tests [13, 14] to study the effects of the hydrochemical environment in locations with stone cultural relics. However, most stone cultural relics have not been affected by the hydrochemical environment for a long time; additionally, environmental changes have not reached levels of extreme dryness or wetness, and they occur relatively slowly. Therefore, further study is needed on the weathering and damage of grotto sandstone caused by the joint action of the hydrochemical environment and daily humidity changes during precipitation.

On this basis, combined with the environmental monitoring data of Longshan Grottoes, rain was taken as a periodic factor, and an accelerated deterioration experiment was conducted indoors. In this study, the macroscopic indicators (mass, wave velocity, surface hardness and tensile strength) of Longshan Grottoes sandstone were evaluated in different hydrochemical environments with daily humidity changes; then, the findings were combined with scanning electron microscopy (SEM) and X-ray diffraction (XRD) analyses to establish damage variables based on porosity. Finally, the damage mechanisms of Longshan Grottoes sandstone in chemical solution and under periodic changes in temperature and humidity were analyzed from qualitative and quantitative perspectives. The findings of this study could provide some references for formulating the follow-up protection program of the Longshan Grottoes and theoretical support for studying the damage mechanisms of sandstone grottoes.

Research program

Research background

The Longshan Grottoes is situated on the summit of Longshan Mountain in southwestern Taiyuan City at the coordinates 112°25′E and 37°43′N (Fig. 1). Data from a temperature and humidity recorder (model: HOBO MX2301A) installed at the grottoes provide the monthly maximum and minimum temperature and humidity values of the Longshan Grottoes in 2022, as shown in Fig. 2. In 2022, the maximum and minimum temperatures in the Longshan area were 48 °C and − 13 °C, respectively; and the maximum and minimum relative humidities were 99% and 8%, respectively.

The main body of the grotto group is on a cliff of the peak of Longshan Mountain. Atmospheric precipitation is the main source of water at Longshan Grottoes. From the data of the China Meteorological Science

Table 1 Hydrological study methods

Scholar	Subject investigated	Soak period (h)	Drying time (h)	Drying temperature (°C)
Bin Du [2]	Red sandstone	24	24	60
Zhanming Shi [3]	Sandstone	24	24	105
Jie Meng [4]	Sandstone	24	/	60
Xiaoshuang Li [5]	Mid-particle sandstone	48	12	50
Huang Zhen [6]	Sandstone	48	24	105
Hexing Zhang [7]	Sandstone	12	12	100
Peng Ying [8]	Compact sandstone	96	24	110
Zilong Zhou [9]	Sandstone	1	> 144	Room temperature (25)
Jingke Zhang [10]	Sandstone	12	12	Room temperature

Fig. 1 Map of the Longshan Grottoes

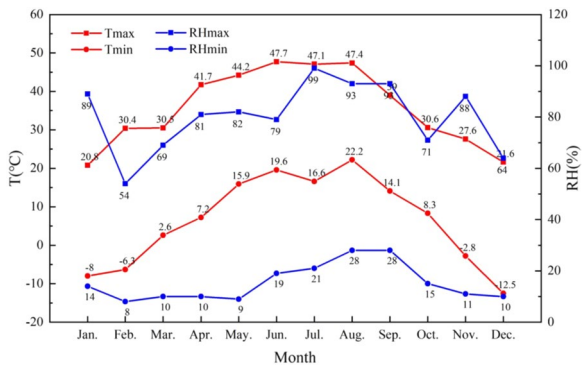

Fig. 2 Maximum and minimum temperature and humidity values of the Longshan Grottoes in 2022

Data Center, the amount and number of days of rainfall in 2022 are found and shown in Fig. 3. The rainfall in 2022 is concentrated in June to August, with a cumulative rainfall of 354 mm in three months, accounting for 71.6% of the annual rainfall. Therefore, the Longshan Grottoes are most affected by rainfall in the summer. There are 68 d of rainfall annually, accounting for 18.6% of all days, which is close to 1/5 of the whole year. The tested samples of rainwater have main cations of Na^+ and Ca^{2+} and primary anions of SO_4^{2-}, Cl^- and HCO_3^-.

Samples on the surfaces of the Longshan Grottoes are collected at different depths for XRD testing. The mineral contents are shown in Fig. 4. The main components of the samples are quartz, albite and clay minerals, with small amounts of epidote.

Sample preparation and test methods

The samples for this experiment were taken from the Longshan Grottoes of Taiyuan, all from the same rock. According to the standard test method for engineering rock masses [15], the samples were processed into cylindrical shapes with diameters of 50 mm and heights of 50 mm. First, samples with obvious defects were removed, and then a nonmetallic ultrasonic detector (Model: NM-4B) was used to screen and group those with similar wave velocities; 10 samples were reserved for the determination of initial mechanical parameters, and the physical parameters of sandstone are shown in Table 2. The samples were divided into 24 groups, each with 3 samples, for deterioration tests.

Testing was conducted in accordance with the standard test method for engineering rock masses [15], and the masses were determined with a hydrostatic balance (model: JA5003). To measure the P-wave velocities of the rock samples, a nonmetallic ultrasonic detector (P-wave transducer with a frequency of 250 kHz, model: NM-4B) was used. The surface hardnesses of the samples were tested with a Riehl hardness tester (Model: BH200C, probe type D). The tensile strengths were assessed through the splitting method with an electrohydraulic universal testing machine (model: CSS-WAW 1000DL). A powder crystal X-ray powder diffractometer (Model: D8 Discover) was used to

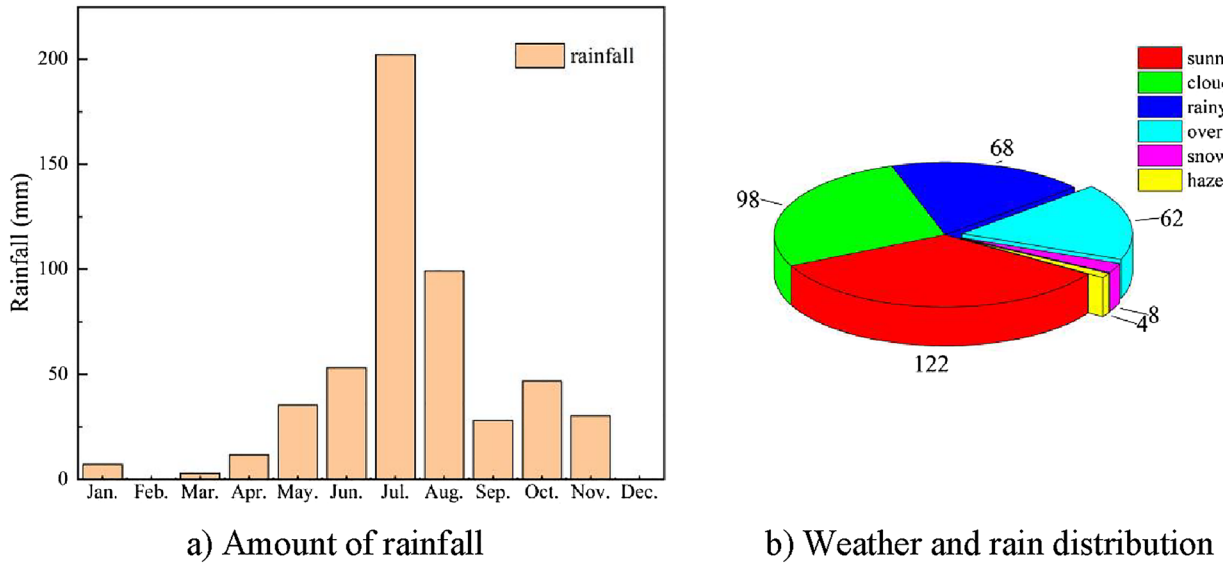

Fig. 3 Amount and number of days of rainfall in 2022: **a**) Amount of rainfall; **b**) Weather and rain distribution

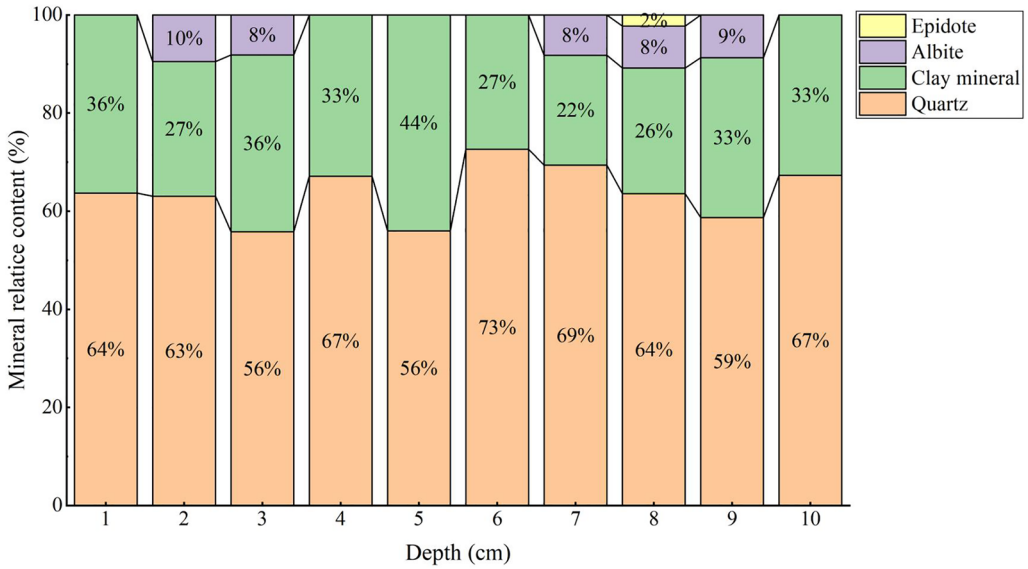

Fig. 4 Semiquantitative X-ray diffraction analysis results of sandstone samples at different hole depths

Table 2 Initial physical parameters of the sandstone

Dry density ($g \cdot cm^{-3}$)	Water absorption rate (%)	Porosity (%)	Richter hardness (HL)	Wave velocity ($km \cdot s^{-1}$)	Compressive strength (MPa)	Tensile strength (MPa)
2.28	4.65	10.81	498	2.214	24.83	2.85

conduct XRD tests, and a scanning electron microscope (model: S-3000 N) was employed to take microscopic photographs.

Deterioration test scheme

1. Soaking solution: according to the identification

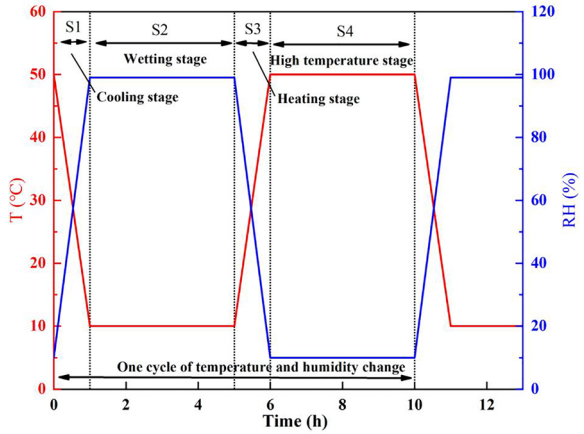

Fig. 5 Schematic diagram of the temperature and humidity change in the dry and wet cycle

results of ion species in rainwater, a 0.1 mol/L solution composed of three sodium salts (Na_2SO_4, NaCl, $NaHCO_3$) was chosen as the soaking solution, with distilled water as the control group.

2. Cyclic test: a fast temperature and humidity variation test box (model: RHPS-408BT) was used to simulate the temperature and humidity changes in the natural environment. After immersing the samples in 4 different solutions for 48 h, they were placed in the test box for 5 temperature and humidity cycles (50 h), with 1 test cycle, as shown in Fig. 5. Combined with summer temperature monitoring data, the test temperatures in the cycle were in the range of 10–50 °C, and the relative humidities were in the range of 10–99%. A degradation test consisting of 48 h of soaking and 5 temperature and humidity cycles was set, and the numbers of test cycles were 3, 6, 9, 12, 15, and 18.
3. Experimental procedure: ① Index determination: after determining the basic physical index of the rock sample, it was placed in an oven at 105 °C for 48 h and then cooled to room temperature; from there, the dry mass, longitudinal wave velocity and surface hardness were measured. ② Cyclic test: after the sample was naturally immersed in different solutions for 48 h, it was placed in the test box to experience altering temperature and humidity conditions. This process was repeated until all samples completed the set number of cycles; the solution was reconfigured every 3 cycles. ③ after the cycled sample dried, the mass, longitudinal wave velocity, surface hardness and tensile strength were tested, and then SEM and XRD tests were performed on the edge surface.

Damage characteristics

Mass change

By determining the mass of the rock samples after different cycles, the macroscopic qualities were characterized by the mass loss rate, as shown in Fig. 6. The results of the changes were as follows: (1) after being subjected to different cycles, the mass loss rates of the 4 groups of samples generally increased with increasing number of cycles. After 3 cycles, the mass loss rate of the rock sample soaked in distilled water was higher than that samples soaked in NaCl solution and in $NaHCO_3$ solution; the mass loss rate of the rock sample soaked in NaCl solution increased. With the increase in the number of cycles, the mass loss rates of the rock samples soaked in NaCl solution and in $NaHCO_3$ solution exceeded those of the sample soaked in distilled water for 6 cycles and 9 cycles; the mass loss rate of the rock sample soaked in Na_2SO_4 solution showed an exponential increase with the increase in the number of cycles; and (2) throughout the cycle, the rates of change in the degrees of mass loss of the samples after soaking in different solutions decreased in the following order: Na_2SO_4 solution, $NaHCO_3$ solution, NaCl solution and distilled water. After 18 cycles, the mass loss rates of the rock samples soaked in distilled water, Na_2SO_4 solution, NaCl solution and $NaHCO_3$ solution reached 0.190%, 1.371%, 0.427% and 0.467%, respectively.

Change in P-wave velocity

The relationship between the number of cycles and P-wave velocity in different solutions is shown in Fig. 7. The results of the changes are as follows. (1) After different cycle times, the P-wave velocities of the rock samples show different degrees of decrease, exhibiting a linear downward trend; and (2) throughout the cycle,

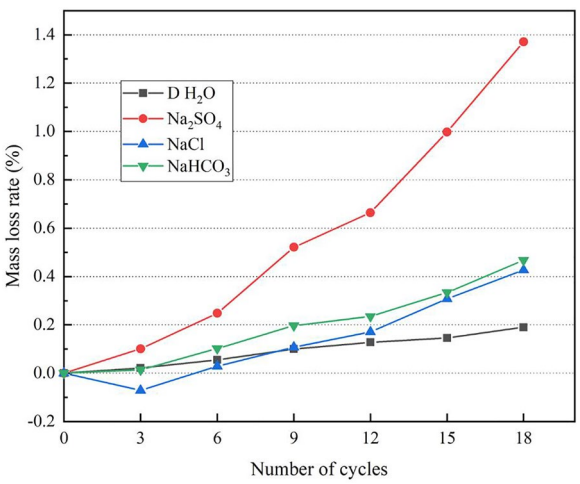

Fig. 6 Relationship between the number of cycles and the rate of mass loss in different solutions

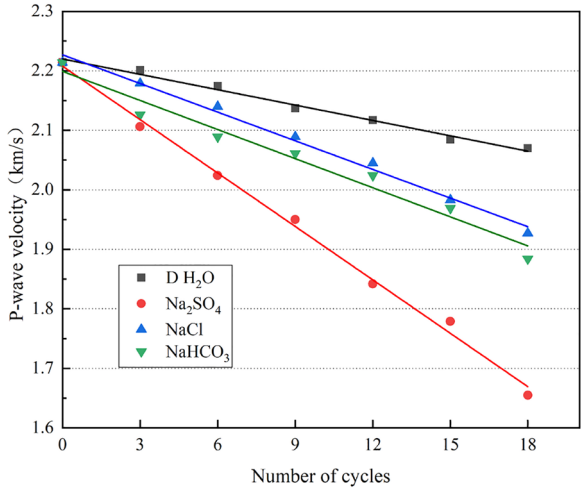

Fig. 7 Relationship between the number of cycles and the P-wave velocity in different solutions

the changes in sample wave velocity after immersion in different solutions range from large to small in the following order: Na_2SO_4 solution, $NaHCO_3$ solution, NaCl solution, and distilled water. The rock samples immersed in distilled water, Na_2SO_4 solution, NaCl solution and $NaHCO_3$ solution after 18 cycles exhibit wave velocities that are 0.144 km/s, 0.559 km/s, 0.287 km/s, and 0.330 km/s smaller than before the test, respectively; and (3) with the same number of cycles, the changes in the wave velocities of the rock samples in the four solution immersion cycles are in the following order: $Na_2SO_4 > NaHCO_3 > NaCl > D\ H_2O$.

Surface hardness changes

After testing the surface hardness of the rock samples after different cycles, as shown in Fig. 8, the results of the changes were found as follows. (1) After different cycles, the surface hardnesses of the samples in four kinds of environments decreased to different degrees, and after three cycles, the hardnesses basically exhibited linear downward trends; (2) throughout the cycle, the surface hardness changes in the samples after immersion in different solutions were in the following descending order: distilled water, Na_2SO_4 solution, $NaHCO_3$ solution, and NaCl solution. After 18 cycles, the surface hardness values of the rock samples immersed in distilled water, Na_2SO_4 solution, NaCl solution, and $NaHCO_3$ solution decreased from 498 HL to 395 HL, 275 HL, 377 HL, and 357 HL, respectively; and (3) in the same cycle, the relationships between the surface hardnesses of the rock samples immersed in the four solutions were in the following order: $Na_2SO_4 > NaHCO_3 > NaCl > D\ H_2O$.

Porosity changes

By testing the porosities of the rock samples after different cycles, the relationships between the cycles and porosities in different solutions were found, as shown in Fig. 9. The results of the variations were as follows. (1) After different numbers of cycles, the porosities of the samples in four kinds of environments increased to different degrees, showing logarithmic upward trends; (2) throughout the cycle, porosity changes in the samples after immersion in different solutions were in the following descending order: Na_2SO_4 solution, $NaHCO_3$ solution, NaCl solution and distilled water. After 18 cycles of immersion in distilled water,

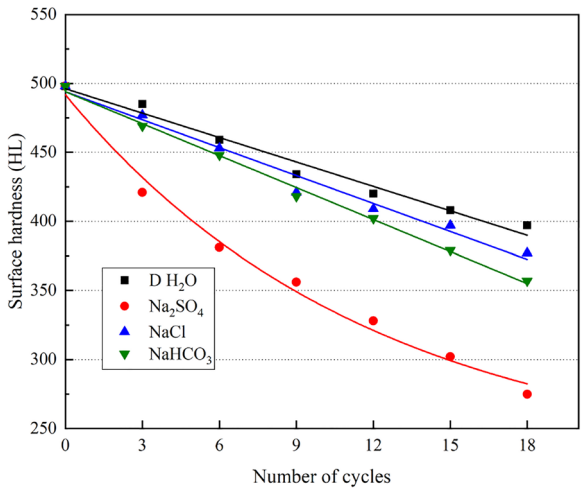

Fig. 8 Relationship between the number of cycles and surface hardness values in different solutions

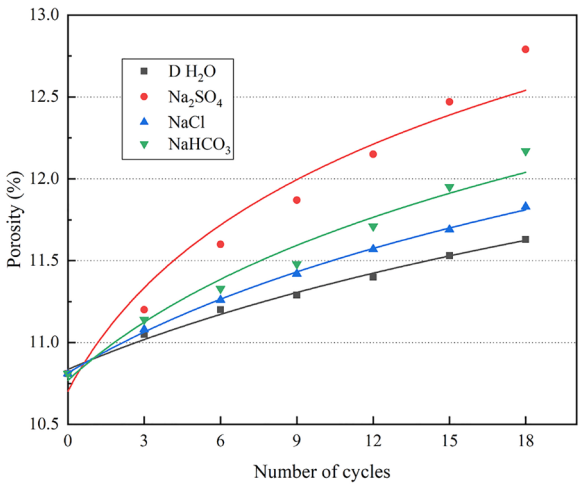

Fig. 9 Relationships between the number of cycles and porosity values in different solutions

Na_2SO_4 solution, NaCl solution, and $NaHCO_3$ solution, the porosities of the samples reached 11.63%, 12.79%, 11.83%, and 12.17%, respectively; and (3) with the same number of cycles, the porosities of the rock samples immersed in the four solutions were in the following order: $Na_2SO_4 > NaHCO_3 > NaCl > D\ H_2O$.

Changes in tensile strength

Brazilian split tests were performed on the rock samples after each cycle, and the destruction modes of sandstone in different solutions are shown in Fig. 10. After the deterioration test, the surface of the sample roughened, and obvious granularity could be felt by touch. Among the rock samples, those soaked in Na_2SO_4 solution exhibited the most obvious change, and those soaked in $NaHCO_3$ solution exhibited the second most obvious change. According to the deterioration effect, the sandstone subjected to tensile failure was divided into two types: (1) tensile failure: cracks were produced and propagated along the loading direction, near the center, and parallel to the loading direction; and (2) composite failure: cracks were inconsistent with the loading direction, deviating to the edge of the rock sample; multiple cracks appeared near the main crack branches. The splitting type of the rock sample after cycling was determined (Table 3), and the composite failure of the rock sample soaked in Na_2SO_4 solution was the most common.

As shown in Fig. 11, the relationship between the number of cycles and the tensile strength in different solutions was similar to that of the surface hardness. The results showed that after different cycles, the tensile strengths of the samples under the four kinds of solutions decreased in different degrees, showing exponential decreasing trends. Throughout the cycle, the changes

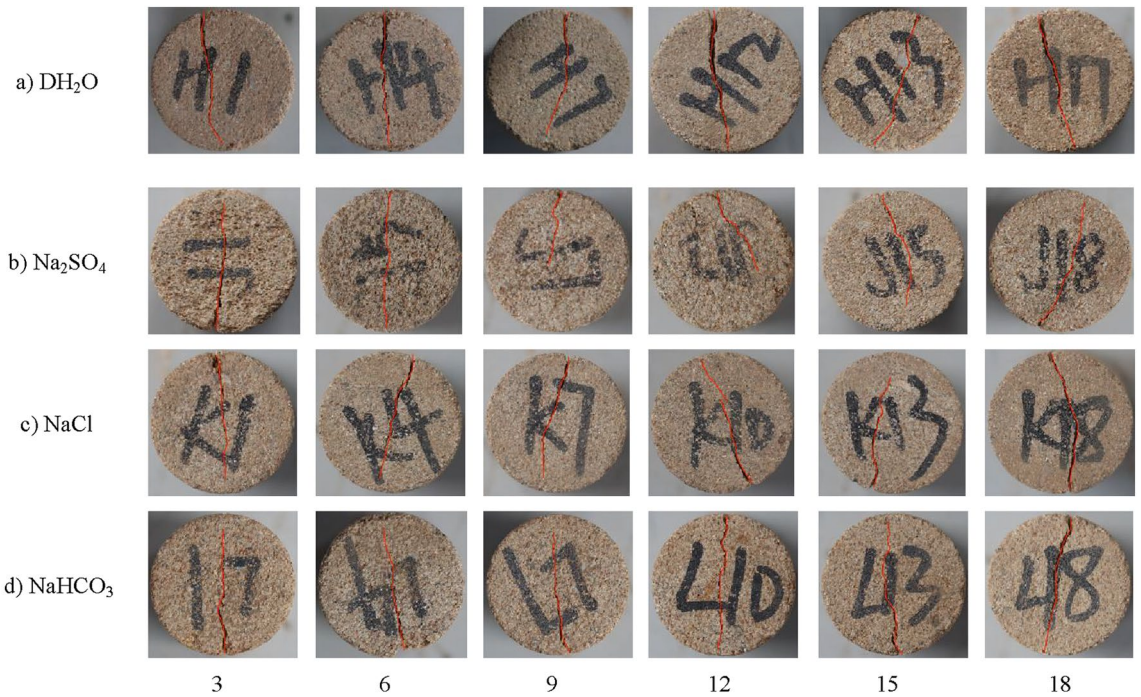

Fig. 10 Brazilian split failure mode of sandstone under dry and wet conditions. (The red line is the crack extension path): **a**) D H2O; **b**) Na2SO4; **c**) NaCl; **d**) NaHCO3

Table 3 Classification of rock sample split types

Solution types	Destruction type		Portion of tensile destruction samples (%)	Portion of composite destruction samples (%)
	Tensile failure	Pull and cut composite damage		
DH_2O	H1–4, H6–7, H9, H12–14, H16–17	H5, H8, H10–11, H15, H18	67	33
Na_2SO_4	J1, J2, J4–5, J11, J13–18	J3, J6–10, J12	61	39
NaCl	L1–4, L6–8, L10–16, L18	L5, L9, L17	83	17
$NaHCO_3$	K1–10, K12–18	K11	94	6

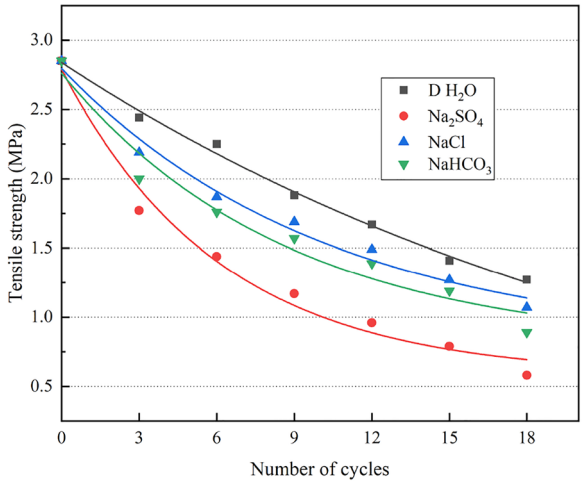

Fig. 11 Relationships between the number of cycles and tensile strength values in different solutions

in the tensile strengths of the samples after immersion in different solutions were in the following descending order: Na_2SO_4 solution, $NaHCO_3$ solution, NaCl solution and distilled water. After 18 cycles of immersion in distilled water, Na_2SO_4 solution, NaCl solution and $NaHCO_3$ solution, the tensile strengths of the rock samples decreased from 2.85 MPa to 1.27 MPa, 0.58 MPa, 1.07 MPa, and 0.89 MPa, respectively. With the same number of cycles, the tensile strengths of the rock samples immersed in the 4 solutions were in the following order: $Na_2SO_4 > NaHCO_3 > NaCl > D\ H_2O$.

Damage mechanism

Qualitative analysis of damage

Microstructural changes

To reveal the changes in the microstructure of Longshan sandstone with different solutions and temperature and humidity cycle changes, 500 × SEM images were taken on the surfaces of the sandstone specimens that underwent 3, 9 and 18 cycles, as shown in Fig. 12. The results were as follows. (1) After soaking in distilled water, holes or cracks were not observed in the sandstone samples after 3 cycles. However, after 9 cycles, linear cracks gradually formed. Finally, after 18 cycles, a substantial number of holes appeared within the samples, causing their structures to soften; (2) for the sandstone samples soaked in Na_2SO_4 solution, after 3 cycles, tiny holes appeared inside the samples and gradually connected to form tiny linear cracks. After 9 cycles, the surface of the sample was chemically corroded, and linear cracks appeared. Finally, after 18 cycles, the holes and linear cracks inside the sample connected and expanded, destroying the sample structure; (3) under the joint action of NaCl solution and temperature and humidity changes, after 3 cycles, small holes appeared on the surface of the sample, and debris was produced. After 9 cycles, the number of holes increased, and after 18 cycles, the holes connected to form linear cracks; and (4) after the sandstone sample was soaked in $NaHCO_3$ solution, the surface showed debris after 3 cycles. After 9 cycles, many holes appeared, and debris was seen everywhere. After 18 cycles, the surface of the sample was severely corroded, and linear cracks expanded. The damage degree of $NaHCO_3$ solution to the rock sample was between that of Na_2SO_4 solution and NaCl solution and higher than that of distilled water.

An analysis of electron microscopy images of samples subjected to different solutions and cycles revealed that the cycles increased the number of holes and the propagation of linear cracks. Furthermore, the degree of deterioration of the sandstone samples increased in the following order: $Na_2SO_4 > NaHCO_3 > NaCl > D\ H_2O$. Notably, after 18 cycles, the deterioration degrees of the sandstone samples in the Na_2SO_4 solution were significantly higher than those in the other three solutions.

Changes in mineral composition

Figure 13 shows the relative content analysis results of rock sample minerals after 18 cycles. Three samples were tested under every operating condition. It can be seen from Fig. 13a that a mineral has multiple diffraction peaks with similar change rules, among which quartz has the most significant diffraction peak, indicating that its content is the highest. Other minerals are mainly albite, calcite and clay minerals. The relative contents of other minerals have also changed, the relative contents of quartz have increased, and the relative contents of albite and clay minerals have decreased. Under the combined action of the chemical solution and the cycle of temperature and humidity changes, the minerals in the rock sample may have undergone some changes. The mineral content of rock samples in four different solution environments has the same variation rule, but the variation amplitude is different to some extent. Among them, the relative content of minerals in Na_2SO_4 solution changed most obviously, the relative content of feldspar decreased by 1.4%, and the relative content of quartz increased significantly by 16.2%. The relative mineral contents in the four solutions were in the order of $Na_2SO_4 > NaHCO_3 > NaCl > D\ H_2O$. This is due to the different degrees of damage to the mineral composition of rock samples caused by different solutions.

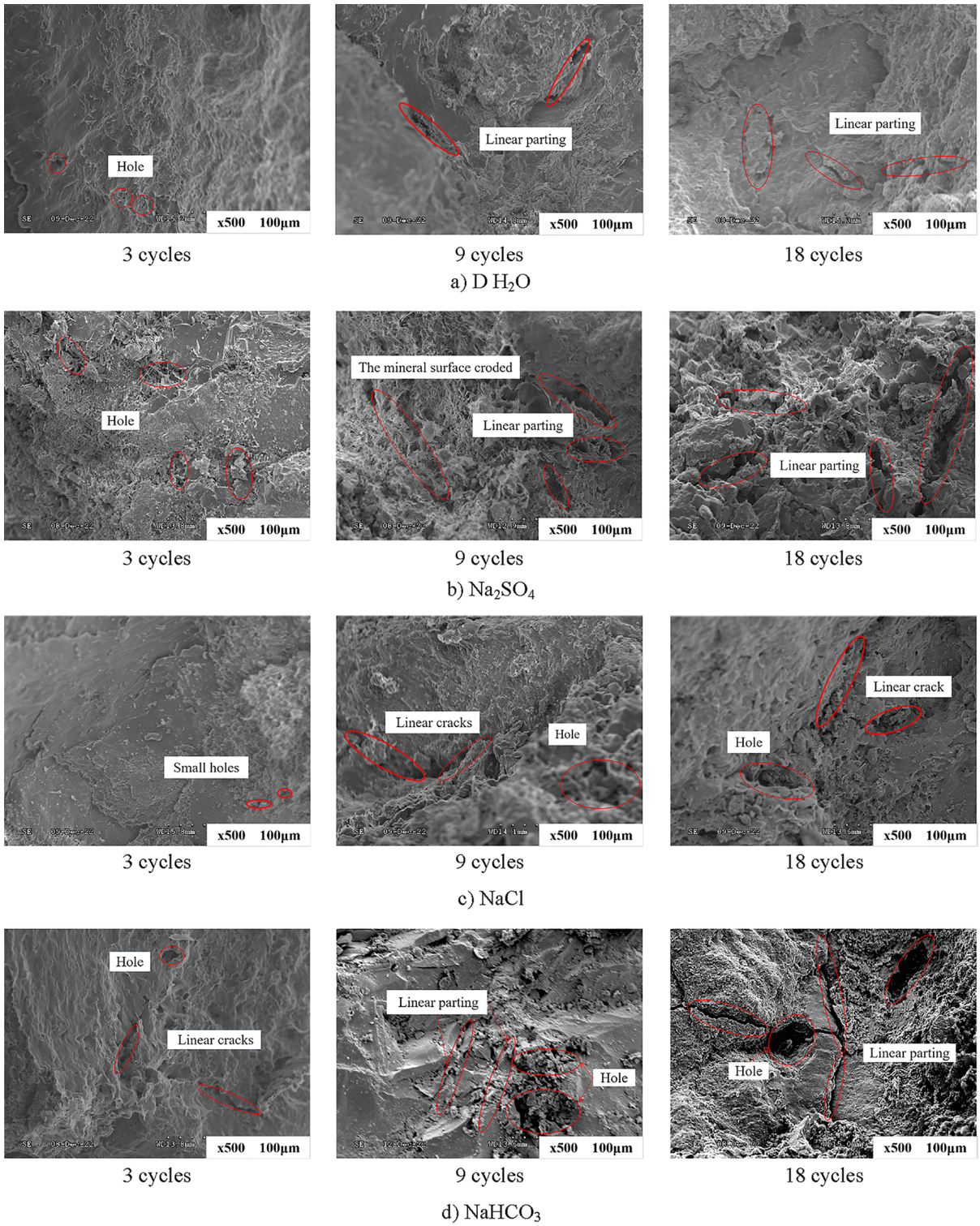

Fig. 12 500×scanning electron microscopy images of samples in different solutions: **a**) D H2O; **b**) Na2SO4; **c**) NaCl; **d**) NaHCO3

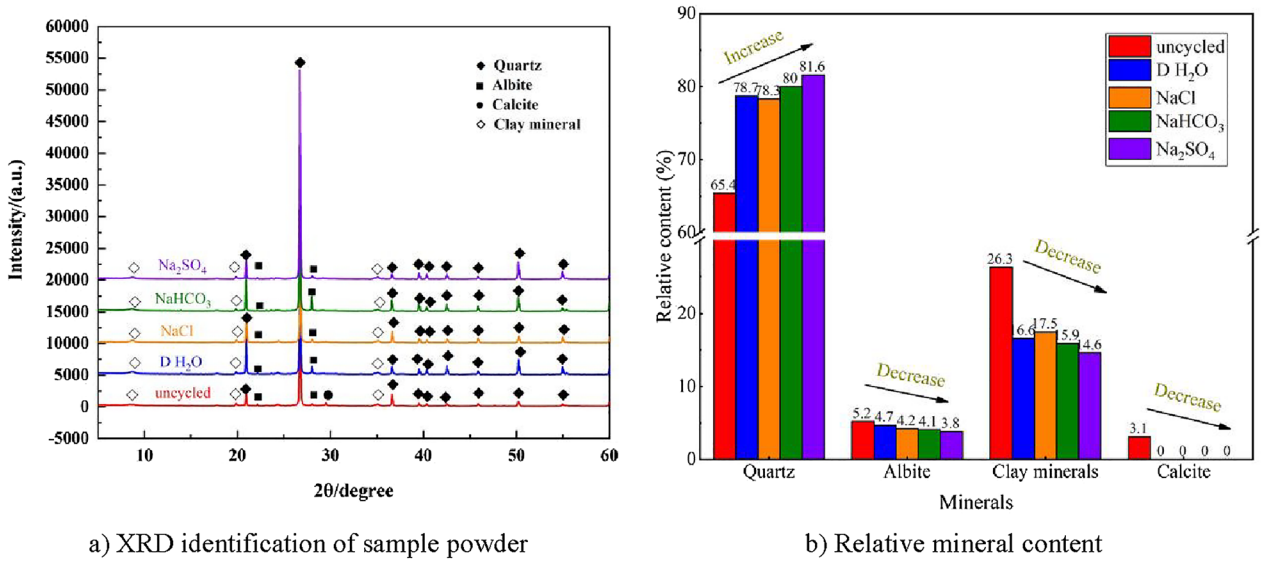

a) XRD identification of sample powder b) Relative mineral content

Fig. 13 Analysis of relative mineral composition of rock samples after 18 cycles: **a**) XRD identification of sample powder; **b**) Relative mineral content

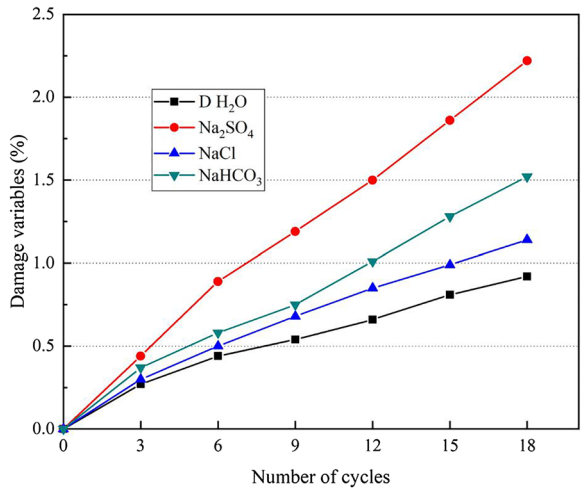

Fig. 14 Sandstone damage variables after different numbers of cycles in different solutions

Damage variable analysis based on porosity changes

Relationships between the damage variable and the number of cycles in different solutions

According to the analysis results of the microstructures and mineral compositions, sandstone saturated with different solutions was subjected to cyclic temperature and humidity changes. The pore damage and the quantity increase and the hole connection were related to the samples. The damage variable D [16] was established by the change in porosity, and the damage degrees of rocks with different chemical solutions and cyclic temperature and humidity changes were quantitatively evaluated. The relationship between the damage variable and porosity was as follows:

$$D = \frac{n_t - n_0}{1 - n_0} = 1 - \frac{1 - n_t}{1 - n_0} \quad (1)$$

where n_0 is the porosity of the original rock and n_t is the porosity of the sample after t cycles.

By calculating the damage variables of different circulation times in different solutions through the above formula and porosity, as shown in Fig. 14, the results were as follows. (1) After circulation, the damage variable D of the four sandstone samples in different solution immersions presented a logarithmic increasing trend with increasing circulation times; (2) throughout the circulation cycle, the change degrees of the damage variables of the samples in different solutions were in the following order: $Na_2SO_4 > NaHCO_3 > NaCl > D\ H_2O$; and (3) after 18 cycles, the damage variables of sandstone samples immersed in distilled water, Na_2SO_4 solution, NaCl solution and $NaHCO_3$ solution increased by 0.92%, 2.22%, 1.14% and 1.52%, respectively.

Relationship between damage variables and macroscopic indexes in different solutions

To investigate the correlations between damage variable D and macroscopic indicators with changing temperature and humidity, the D values of sandstone samples in the four solutions and with the temperature and humidity cycle changes were fitted with the change rates of wave velocity, surface hardness and tensile strength, and the regression results are shown

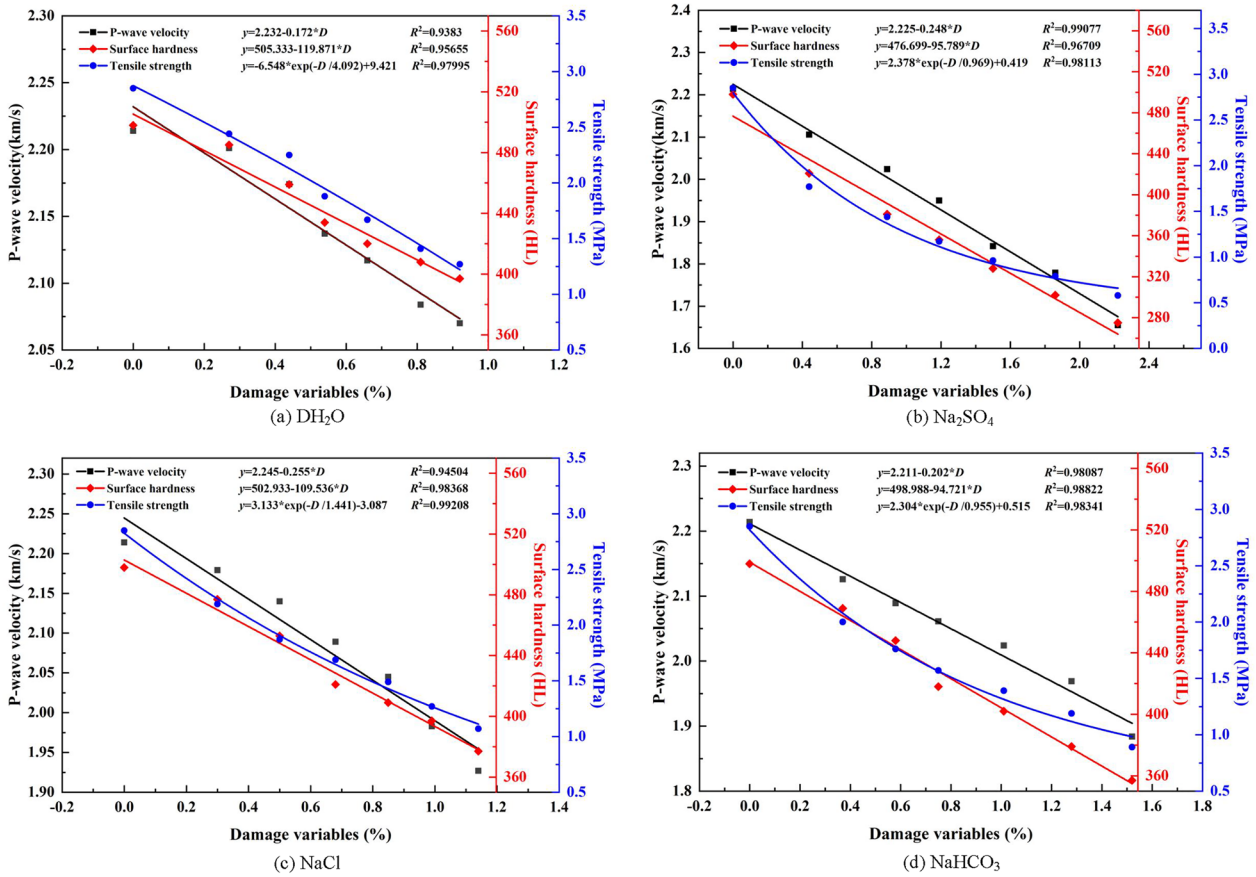

Fig. 15 Relationships between macroscopic test indexes and damage variables in different solutions: **a**) D H2O; **b**) Na2SO4; **c**) NaCl; **d**) NaHCO3

in Fig. 15. The results were as follows. (1) In the four solutions, there were linear relationships between the wave velocity change rate and the damage variable *D* and between the surface hardness and the damage variable *D*; the tensile strength and the damage variable *D* showed an exponential relationship; and (2) the correlation coefficients of the fitting functions were all above 0.945, and the fitting degrees of the macroscopic physical parameters and damage variables were good, indicating that there was an obvious quantitative relationship between the macroscopic damage indicators of samples in different solutions and porosities.

Damage mechanism

The above test results showed that after periodic changes in the temperature and humidity of sandstone samples immersed in different solutions, the macroscopic properties, microstructures and compositions of the samples are cumulatively damaged with the increase in the number of cycles. The damage of the samples after cycling is caused by the differential combination of three effects—hydrolysis, erosion and salt crystallization—resulting in different internal pore characteristics, numbers and connections.

The damage to the sandstone after the cyclical variations in temperature and humidity in distilled water is mainly caused by hydrolysis. Feldspar minerals, such as albite, in sandstone are hydrolyzed in solution, and albite reacts with H_2O to form Na^+, $Al(OH)_4^-$ and H_4SiO_4 [17]. The reaction is shown in Eq. (2). Calcite is unstable in neutral to alkaline solutions with pH values of 7–8.5 easily hydrolyses and migrates [18]. The hydration process is shown in Eq. (3). In addition, certain clay minerals are lost, causing holes on the surfaces and insides, cracks, connections, and erosion on the surfaces of the samples. This finding is consistent with the SEM photos after 3, 9 and 18 cycles and corresponds to the changes in the relative contents of minerals detected by XRD.

$$NaAlSi_3O_8 + 8H_2O = Al(OH)_4^- + Na^+ + 3H_4SiO_4 \quad (2)$$

$$CaCO_3(Calcite) + H_2O + CO_2 = Ca(HCO_3)_2 \quad (3)$$

The damage caused by NaCl solution to rocks is more significant than that of distilled water. After the experiment, there is no notable change in the outward appearance of the rock sample, but its mass increases after 3 cycles. This increase may occur due to salt sticking to or permeating the sample. Nevertheless, an alteration in mass is not the only indicator of rock sample damage [19]. Decreases in hardness and wave velocity reveal that the surface and interior of the sample have been damaged. NaCl transports water inside the pores of the rock mass, which crystallizes, and fresh salt crystals are precipitated on the fractured rock surface; salt redistribution and progressive accumulation eventually lead to rock sample destruction [20]. According to the SEM detection results, the degrees of pore and crack development on the microstructure of the rock sample are slightly greater than those of the distilled water sample; the relative content of albite in the XRD semiquantitative analysis of minerals decreases to a greater extent than that of the distilled water, indicating that the presence of Cl^- can accelerate the damage of rocks caused by alternating temperature and humidity values.

The destructive effects of $NaHCO_3$ solution on sandstone samples following drying and wetting processes are primarily caused by hydrolysis and salt erosion. After 3 cycles, the rock sample experiences less mass loss than it does in distilled water. This reduced loss occurs due to the effect of salt; however, $NaHCO_3$ has a more damaging effect on the rock sample, and its mass loss rate is higher than that of the rock sample in distilled water after 6 cycles. Long-term dissolution increases the number of pores and cracks, resulting in clay mineral loss. Last, due to chemical dissolution, the degrees of development of pores and cracks within the microstructure and the relative contents of minerals in semiquantitative XRD mineral analysis are greater than those in distilled water and NaCl solution.

After cyclic changes in temperature and humidity on the sandstone samples in Na_2SO_4 solution, the cumulative damage of the samples is mainly caused by the joint action of hydrolysis, erosion and salt crystallization. As temperatures decrease during the cycle, Na_2SO_4 crystals in the pores of sandstone absorb water to form $Na_2SO_4{\cdot}10H_2O$ [21], thus increasing the crystal volume and damaging the rock sample. Adverse temperatures and humidity accelerate the hydration–dehydration process [22], thereby enlarging the pore size. Pressure crystallization depends on the rock sample saturation process and the pore size [23]. This repeated action gradually increases the sizes of the large pores, resulting in a greater damage degree for the rock sample in Na_2SO_4 solution than for those soaked in other solutions. The expansion of internal pores and cracks roughens the surface of the rock sample and decreases its surface hardness from the inside to the outside.

In summary, the damage mode of sandstone after immersion in different solutions and changing the environmental cycles of temperature and humidity is composed of two parts: one part is the damage when soaking the solution, and the other part is the damage caused by temperature and humidity changes to the rock sample. The damage to sandstone during immersion is mainly caused by the hydrolysis of feldspar and the loss of clay minerals, as described in detail above. In addition to salt crystallization, the alternating changes in temperature and humidity cause the salt to combine with water molecules and fall off, resulting in the repeated expansion of volume and the loosening and removal of these particles from the rock surface. This phenomenon causes salts and minerals to interact to form soluble salts that are relatively stable under certain conditions, and volume shrinkage destroys the intergranular connection.

For sandstone samples in different solutions, the sample damage in distilled water is mainly caused by feldspar hydrolysis, water scouring, and clay mineral expansion and disintegration. The rock samples in the salt solution are affected by soluble salts. For rock samples in NaCl solution and $NaHCO_3$ solution, these soluble salts will enter the pores of rock samples and destroy the internal structure. $NaHCO_3$ solution is generally weakly alkaline, which will increase the degree of feldspar hydrolysis. The salt crystallization of $NaHCO_3$ and Na_2SO_4 occurred with the change in temperature condition, which caused damage to the rock samples, but the crystallization effect of Na_2SO_4 was stronger than that of $NaHCO_3$. The above explains is why the sandstone deterioration degree follows the order of: $Na_2SO_4 > NaHCO_3 > NaCl > D\ H_2O$.

Conclusion

In this study, the effects of water chemistry and cyclic changes in temperature and humidity on the weathering of sandstone cultural relics are studied by simulating summer rain and weather changes in an indoor experimental setup. The conditions are milder in this experimental work are milder than those considered in other experiments, but the deterioration effects are still significant, and the following conclusions are obtained.

1. Sandstone samples immersed in different solutions are damaged to different degrees under changes in temperature and humidity. The mass, wave velocity, surface hardness and tensile strength values of the sandstone decrease with the increase in the number of cycles; most indicators take 3 cycles as the node, and the rate of change is divided into two stages. The macroparameters have different responses to

the effect of deterioration, and the trends of hardness and tensile strength are consistent. The decrease in each physical index is in the following order: $Na_2SO_4 > NaHCO_3 > NaCl > D\ H_2O$.

2. Under periodic changes in temperature and humidity, the porosities of rock samples after immersion in different solutions increase with increasing cycles, and the internal structure shows the phenomenon of increasing holes and extending linear cracks; in addition, the mineral content changes, which is manifested as relative decreases in calcite and feldspar minerals, the loss of clay minerals, and the increase in quartz relative content.
3. The damage variable *D*, which is established based on the porosity rate, increases logarithmically with increasing circulation times; the degree of change in the damage variable *D* after different solution immersions is in the following order: $Na_2SO_4 > NaHCO_3 > NaCl > D\ \ H_2O$. The damage variable *D* has a linear relationship with the rate of change in the wave velocity and the surface hardness and an exponential relationship with the tensile strength; the corresponding R^2 is values are at least 0.945.
4. The essential nature of the damage to the Longshan Grottoes sandstone is caused by a combination of actions, such as the feldspar hydrolysis, chemical erosion, salt crystallization and dissolution, clay mineral expansion, and water scouring and softening, resulting in linear pores and holes inside the rock and rapid increases in the number and connection of the holes.

Acknowledgements
We thank our colleagues at Northwest Research Institute Limited Company of China Railway Engineering Corporation for their great help in this work. We thank the editors for their patience processing our manuscript. The anonymous reviewers are gratefully acknowledged for their careful and insightful reviews.

Author contributions
Conceptualization, BS and KC; methodology, XL and NP; validation, NP; formal analysis, XL, J.H. and R.C.; investigation, CJ; writing—original draft preparation, XL; writing—review and editing, BS, KC and NP; funding acquisition, KC and NP. All authors have read and agreed to the published version of the manuscript.

Funding
This work was supported by the National Natural Science Foundation of China (No. 52068050, No. 41562015, No. 51808246), the Program for Changjiang Scholars and Innovative Research Team in University of Ministry of Education of China (No. 2017IRT17_51) and National Key Research and Development Program of China (No. 2019YFC1520500).

Availability of data and materials
Not applicable.

Declarations

Competing interests
The authors declare no competing interests.

Received: 5 May 2023 Accepted: 5 August 2023
Published online: 15 August 2023

References

1. Sun B, Li XY, Cui K, Peng NB, Hong J, Chen R, Jia C. Study on the characteristics of damaged sandstone in the Longshan Grottoes using water chemistry and freeze-thaw cycling. Minerals. 2023;13(3):430.
2. Du B, Cheng Q, Miao L, Wang J, Bai H. Experimental study on influence of wetting-drying cycle on dynamic fracture and energy dissipation of red-sandstone. J Build Eng. 2021;44:102619.
3. Shi Z, Li J, Zhao Y. Study on damage evolution and constitutive model of sandstone under the coupled effects of wetting-drying cycles and cyclic loading. Eng Fract Mech. 2021;253:107883.
4. Meng J, Li CD, Zhou JQ, Zhang ZH, Yan SY, Zhang YH, Huang DW, Wang GH. Multiscale evolution mechanism of sandstone under wet-dry cycles of deionized water: from molecular scale to macroscopic scale. J Rock Mech Geotech Eng. 2023;15(5):1171–85.
5. Li X, Peng K, Peng J, Hou D. Experimental investigation of cyclic wetting-drying effect on mechanical behavior of a medium-grained sandstone. Eng Geol. 2021;293: 106335.
6. Huang Z, Zhang W, Zhang H, Zhang JB, Hu ZJ. Damage characteristics and new constitutive model of sandstone under wet-dry cycles. J Mt Sci. 2022;19(7):2111–25.
7. Zhang HX, Lu K, Zhang WZ, Li DL, Yang GL. Quantification and acoustic emission characteristics of sandstone damage evolution under dry–wet cycles. J Build Eng. 2022;48:103996.
8. Ying P, Zhu Z, Ren L, Deng S, Niu CY, Wan DY, Wang W. Deterioration of dynamic fracture characteristics, tensile strength and elastic modulus of tight sandstone under dry-wet cycles. Theoret Appl Fract Mech. 2020;109(3–4):102698.
9. Zhou ZL, Cai X, Ma D, Chen L, Wang SF, Tan LH. Dynamic tensile properties of sandstone subjected to wetting and drying cycles. Constr Build Mater. 2018;182:215–32.
10. Zhang JK, Li Z, Li L, Liu JH, Liu D, Shao MS. Study on weathering mechanism of sandstone statues in Southwest China: example from the sandstone of Niche of Sakyamuni Entering Nirvana at Dazu Rock Carvings. Nat Hazards. 2021;108(1):775–97.
11. Dehestani A, Hosseini M, Beydokhti AT. Effect of wetting–drying cycles on mode I and mode II fracture toughness of sandstone in natural (pH=7) and acidic (pH=3) environments. Theoret Appl Fract Mech. 2020;107:102512.
12. Li H, Zhong ZL, Liu XR, Sheng Y, Yang DM. Micro-damage evolution and macro-mechanical property degradation of limestone due to chemical effects. Int J Rock Mech Min Sci. 2018;110:257–65.
13. Lin Y, Zhou KP, Gao RG, Li JL, Zhang J. Influence of chemical corrosion on pore structure and mechanical properties of sandstone. Geofluids. 2019;2019:7320536.
14. Cui K, Gu X, Wu GP, Li H, Du ZZ. Dry-wet damage characteristics and mechanism of metamorphic sandstone carrying Helan mouth's rock paintings under different conditions. Chin J Rock Mech Eng. 2021;40(06):1236–47 (**in Chinese**).
15. The National Standards Compilation Group of Peoples Republic of China. GBT50266—2013 Standard for test method of engineering rock mass. Beijing: China Planning Publishing House; 2013.
16. Ding WX, Feng XT. Study on chemical damage effect and quantitative analysis method of mesostructure of limestone. Chin J Rock Mech Eng. 2005;24(8):128–1288 (**in Chinese**).
17. Cai YY, Yu J, Fu GF, Li H. Experimental investigation on the relevance of mechanical properties and porosity of sandstone after hydrochemical erosion. J Mt Sci. 2016;13:2053–68.

18. Krawczyk WE, Ford DC. Correlating specific conductivity with total hardness in limestone and dolomite karst waters. Earth Surf Process Landf. 2006;31:221–34.
19. Lisci C, Pires V, Sitzia F, Mirão J. Limestones durability study on salt crystallisation: an integrated approach. Case Stud Constr Mater. 2022;17:e01572.
20. Qu JJ, Zhang MQ, Zhang WM, Wang YP, Dai FN, Zhang HY, Zeng ZZ. A preliminary study on weathering process of salt in rock body at Mogao Grottes, Dunhuang. Sci Geogr Sin. 1995;15(02):182–7.
21. Rodriguez-Navarro C, Doehne E, Sebastian E. How does sodium sulfate crystallize? Implications for the decay and testing of building materials. Cem Concr Res. 2000;30(10):1527–34.
22. Steiger M, Asmussen S. Crystallization of sodium sulfate phases in porous materials: the phase diagram Na_2SO_4·H_2O and the generation of stress. Geochim Cosmochim Acta. 2008;72(17):4291–306.
23. Benavente D, García Del Cura MA, Bernabeu A, Ordonez S. Quantification of salt weathering in porous stones using an experimental continous partial immersion method. Eng Geol. 2001;59:313–25.

Publisher's Note